minerals

MDPI

Article

Magnetic and Pedological Characterization of Soil Profiles from Weakly Magnetic Clastic Rock in Yunnan Province, China

Xinglin Huang [1,2], Meichen Wang [1], Xiaoling Zhang [1,3,4,*], Haixia Li [1,3,4,*], Shiyu Li [5], Hongzhan Liu [3,4,6], Jianjie Wang [1] and Guicai Yu [1]

[1] Faculty of Land Resources Engineering, Kunming University of Science and Technology, Kunming 650500, China; huangxinglin580@gmail.com (X.H.); 15733530502@163.com (M.W.); 18120266569@163.com (J.W.); 18087949820@163.com (G.Y.)
[2] Yunnan Celex Technology Co., Ltd., Kunming 650500, China
[3] Key Laboratory of Geohazard Forecast and Geoecological Restoration in Plateau Mountainous Areas, Ministry of Natural Resources, Kunming 650093, China; 20040090@kust.edu.cn
[4] Key Laboratory of Geological Hazard Prediction and Early Warning and Ecological Protection and Restoration in the Plateau Mountainous Areas of Yunnan Province, Ministry of Natural Resources of the People's Republic of China, Kunming 650000, China
[5] School of Ecology and Environmental Science & Yunnan Key Laboratory for Plateau Mountain Ecology and Restoration of Degraded Environments & International Cooperative Center of Plateau Lake Ecological Restoration and Watershed Management of Yunnan, Yunnan University, Kunming 650500, China; lisy@ynu.edu.cn
[6] Yunnan Geology and Mining Engineering Survey Group Co., Ltd., Kunming 650000, China
* Correspondence: zhxl@kust.edu.cn (X.Z.); lhx4519@163.com (H.L.)

Abstract

In this study, representative soil profiles developed on clastic rock parent materials in Yunnan Province were investigated to elucidate the formation mechanisms of soil magnetic properties under weakly magnetic parent material conditions and to evaluate the response of magnetic enhancement to chemical weathering and pedogenic differentiation. A combination of environmental magnetic measurements, bulk geochemical analyses, weathering index calculations, and ternary diagram discrimination was applied to characterize soil magnetic behavior, magnetic grain size distribution, and chemical weathering processes. The results show that the clastic rock parent materials exhibit overall low magnetic intensities, with low-frequency magnetic susceptibility (χ_{lf}) ranging from 2.543 $\times$ 10^{-8} m^3/kg to 595.652 $\times$ 10^{-8} m^3/kg. Under this weakly magnetic background, soils in the study area display pronounced pedogenic magnetic enhancement, with magnetic parameters showing clear and systematic vertical differentiation along soil profiles, indicating that soil magnetic signals are primarily controlled by pedogenesis. The frequency-dependent susceptibility (χ_{fd}%) generally falls within the range of 5.403%–17.574%, with a mean value of 12.898%, suggesting a substantial contribution from fine-grained magnetic particles. Magnetic grain size diagnostics further indicate that newly formed superparamagnetic (SP) and stable single-domain (SSD) particles generated during pedogenesis dominate the magnetic enhancement signal. The results of the Chemical Index of Alteration (CIA) indicate that approximately 78% of the profiles reach the strong weathering category (CIA > 85), while only 22% fall into the moderate weathering category (CIA: 65–85). Correlation analyses further reveal that grain-size-sensitive magnetic ratios (e.g., χ_{fd}%, χ_{ARM}/SIRM) exhibit a strong correspondence with chemical weathering intensity indicators. These findings suggest that, under weakly magnetic parent material conditions, pedogenically induced magnetic enhancement can be more readily identified and quantitatively assessed. The integration of environmental magnetism and geochemical approaches, therefore, provides a robust framework for investigating pedogenic differentiation and supports high-resolution paleoenvironmental reconstruction in regions dominated by weakly magnetic parent materials.

Check for updates

Academic Editors: Jajati Mandal, Andrew S. Hursthouse, Mohammad Mahmudur Rahman and Juan Manuel Martín-García

Received: 14 January 2026
Revised: 1 March 2026
Accepted: 9 March 2026
Published: 12 March 2026

Copyright: © 2026 by the authors. Licensee MDPI, Basel, Switzerland. This article is an open access article distributed under the terms and conditions of the Creative Commons Attribution (CC BY) license.

Keywords: weakly magnetic clastic rocks; magnetic characteristics; pedogenesis; soil magnetism; chemical weathering

1. Introduction

As a fundamental constituent of terrestrial ecosystems, soil performs indispensable functions in agricultural production, contaminant filtration, and atmospheric CO_2 regulation while simultaneously serving as a definitive terrestrial archive for paleoenvironmental history [1,2]. Meanwhile, soil is a naturally magnetic material, exhibiting magnetic properties that are attributed to the mineralogical types, concentrations, and grain size distributions of the main iron oxides (e.g., magnetite, maghemite, hematite, and goethite) [3,4]. A wide range of methods, such as geochemical analysis [5], microscopic analysis [6], and spectroscopic and thermal analysis [7,8], have been applied to investigate soil magnetic properties. Compared with such methods, environmental magnetism has been increasingly employed to study pedogenesis in Quaternary sediments, paleoclimatic evolution, and the impacts of human activities owing to its high sensitivity, analytical efficiency, non-destructive nature, and relatively low cost [7,9,10]. Through systematic analysis of soil magnetic characteristics with the environmental magnetism method, it is possible to constrain sediment provenance, infer the physicochemical conditions of soil formation, and quantitatively reconstruct environmental parameters such as past precipitation and temperature [11,12].

In well-developed aerobic soils, pedogenic processes commonly lead to pronounced magnetic enhancement, which is a phenomenon widely referred to as the "pedogenic enhancement mechanism" [13]. This process is primarily associated with the transformation and neoformation of fine-grained ferrimagnetic minerals, primarily maghemite or magnetite, derived from primary iron-bearing minerals under alternating wet–dry conditions and potential biogeochemical influences [3,14]. Consequently, the accumulation of pedogenically derived magnetic minerals constitutes the main source of enhanced soil magnetism, highlighting the strong control exerted by pedogenesis on soil magnetic property [15,16]. Previous studies have demonstrated that soil magnetic parameters provide robust indicators of pedogenic intensity [3,17]. Specifically, low-frequency magnetic susceptibility (χ_{lf}) is generally used to represent the overall abundance of ferrimagnetic minerals, whereas frequency-dependent susceptibility (χ_{fd}) and percentage frequency-dependent susceptibility (χ_{fd}%) are particularly effective in diagnosing pedogenically formed superparamagnetic (SP) particles [18,19]. Additionally, anhysteretic remanent magnetization susceptibility (χ_{ARM}) shows a high sensitivity to stable single-domain (SSD) grains, while saturation isothermal remanent magnetization (SIRM) reflects the concentration of magnetic minerals excluding the SP fraction [19].

Complementary to magnetic parameters, soil geochemical composition and pedogenic indices provide independent and robust evidence for diagnosing the stages and intensity of soil development [18]. Major element compositions directly record the decomposition pathways of silicate minerals, elemental mobility, and residual enrichment during weathering and leaching processes, thereby reflecting both the intensity and nature of pedogenesis [20]. Under intense chemical weathering, alkali metals (e.g., Na and K) and alkaline earth metals (e.g., Ca and Mg) are readily released from the silicate mineral lattice and leached via runoff, whereas less mobile Fe and Al oxides gradually accumulate in the residual fraction, forming the characteristic subtropical "Si loss and Al enrichment" geochemical signature [21,22]. Based on these elemental behaviors, Harnois [23], Nesbitt [24], and Young [25] proposed the Chemical Index of Weathering (CIW) and the Chemical Index of Alteration (CIA) to

quantitatively assess the degree of soil weathering, with CIA values between 85 and 100 typically indicating the onset of intense chemical weathering [24,25]. Moreover, the iron liberation index (the ratio of free iron (Fed) to total iron (Fet)) effectively reflects the release of iron from primary minerals and its redistribution and accumulation during pedogenic processes [26]. Although soil magnetic enhancement is often attributed to iron oxidation and reorganization, the relationship between magnetic parameters and geochemical indices may vary across different stages of weathering, underscoring the necessity of integrating magnetic and geochemical approaches [22,27]. Therefore, combining magnetic indicators with geochemical parameters provides a significant understanding of the material basis and evolutionary mechanisms of pedogenesis.

It has been suggested that soil magnetic properties are jointly controlled by both pedogenic processes and parent material characteristics [28]. In regions with diverse lithologies and pronounced spatial heterogeneity, distinguishing between lithogenic magnetic background and pedogenic magnetic enhancement represents a prerequisite for the reliable application of environmental magnetism in soil process studies and paleoenvironmental reconstruction. Yunnan Province is characterized by complex geological settings and a wide distribution of weakly magnetic sedimentary rocks, particularly sandstones, mudstone and shales [29,30]. Soils developed on such parent materials exhibit inherently low magnetic backgrounds, under which magnetic enhancement induced by pedogenic weathering processes becomes relatively amplified. This provides an advantageous natural setting for detecting, isolating, and quantifying pedogenic controls on soil magnetism [29,30]. However, the sensitivity and applicability of different magnetic parameters in weakly magnetic systems remain insufficiently constrained.

Located on a low-latitude plateau under the combined influence of the East Asian and South Asian monsoons, Yunnan Province represents a typical subtropical warm–humid pedogenic region [31]. Intense chemical weathering under these climatic conditions has profoundly reshaped soil material composition and magnetic signatures. Despite this, systematic investigations into the evolution of magnetic particles in weakly magnetic soils across varying pedogenic intensities, as well as on the effectiveness of magnetic parameters as quantitative indicators of pedogenic processes, remain limited.

To address these issues, this study focuses on typical soils developed on weakly magnetic clastic rocks in Yunnan Province. Multiple representative soil profiles were systematically sampled and analyzed using an integrated approach combining environmental magnetic measurements, bulk geochemical analysis, and multivariate statistical methods. The objectives of this study are to (1) characterize the fundamental magnetic properties and their vertical distribution patterns along the soil–parent material continuum; (2) quantify the relationships between diverse magnetic proxies (χ_{lf}, χ_{fd}, χ_{fd}%, χ_{ARM} and SIRM) and major geochemical oxides (SiO_2, Al_2O_3, CaO and Fe_2O_3), as well as key pedogenic indices (CIA, CIW, Sa, and Saf); and (3) elucidate pedogenic magnetic enhancement mechanisms specific to weakly magnetic lithologies and evaluate the feasibility of using magnetic parameters as reliable quantitative indicators of regional chemical weathering intensity in weakly magnetic clastic parent material systems. This study aims to refine environmental magnetic models applicable to low magnetic background regions and to provide a robust scientific framework for pedogenesis research and high-resolution paleoenvironmental reconstruction in subtropical plateau environments.

2. Study Area

As shown in Figure 1a, the study area is located in Yunnan Province, Southwest China (21.8–29.15° N, 97.31–106.11° E), at a mean hypsometric elevation of approximately 1713 m. The climate of this region shows significant diversity under the influence of the

Asian monsoon system, exhibiting a mean annual temperature of nearly 18 °C and mean annual precipitation spanning 1200–1700 mm. Precipitation is strongly seasonally concentrated, with 85%–90% of annual moisture influx between May and October, exhibiting the quintessential monsoon hydroclimatic characteristic. Additionally, driven by the synergistic effects of a vast latitudinal span and pronounced topographic variability, this study area shows a clear north–south climatic zonation: the southern extremity is defined by perennially high-temperature tropical rainforest regimes, which transition northward into subtropical, temperate, and frigid–alpine zones as the monsoonal influence progressively attenuates and seasonal fluctuations intensify. The geomorphic landscape is remarkably heterogeneous, comprising alpine massifs, alluvial plains, intermontane basins, and deeply incised canyons; the overall terrain follows a staircase-like descent from the high-altitude northwest to the low-lying southeast.

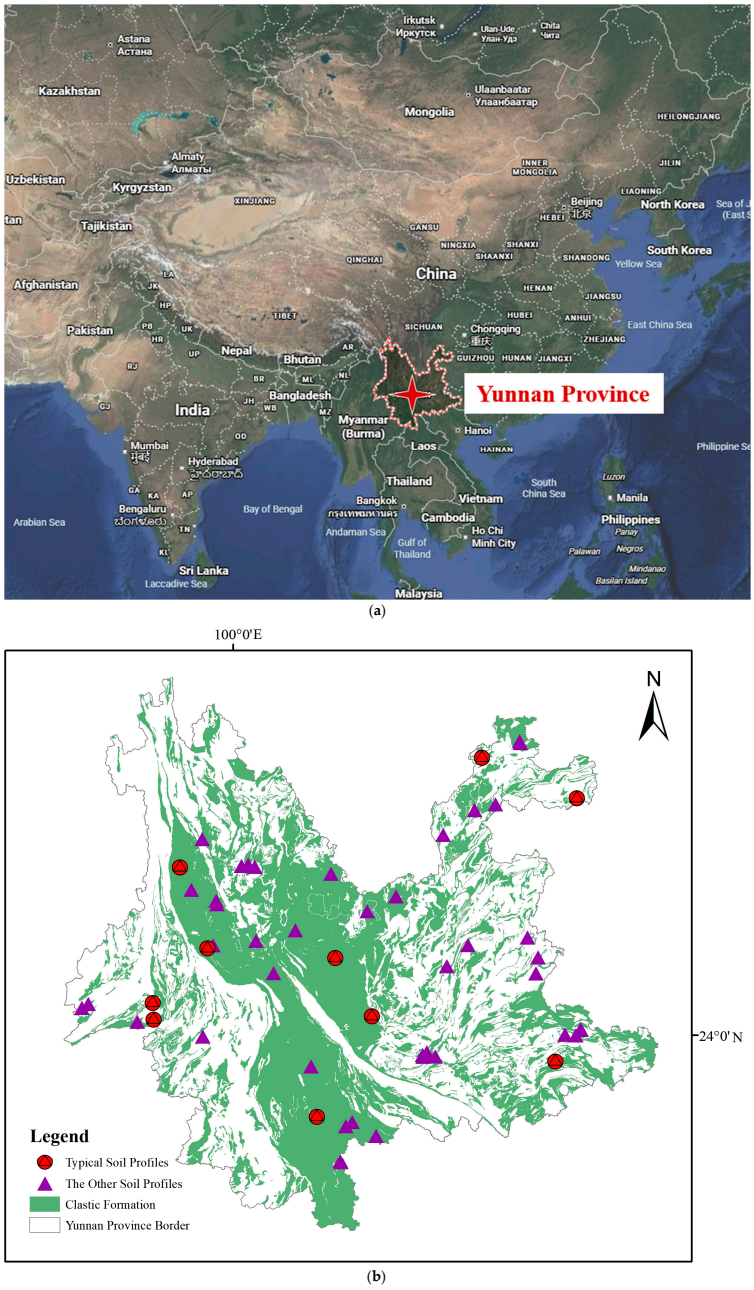


Figure 1. Location of the study area and distribution of soil sampling sites in Yunnan Province, southwestern China. (**a**) Geographic location of Yunnan Province within China; (**b**) Distribution of soil profile sampling sites.

Overall, under the potential influence of climate, relief, biodiversity, and geological substrates, the region has fostered an exceptionally diverse soil system. Geologically, the soil profiles investigated in this study were developed over a remarkably broad range of stratigraphic sequences, spanning from the Mesoproterozoic (Pt_2) to the Neogene (N). However, the majority of the sampling sites are concentrated on Mesozoic clastic rocks, which are the most representative "red beds" of the Yunnan Plateau. Specific stratigraphic units include the Middle Jurassic Shezi Formation (J_2s), Lower Cretaceous Jingxing (K_1j) and Guankou (K_1g) Formations, and various Triassic sequences (e.g., T_1f, T_2gb). These formations are predominantly composed of purplish-red to brownish-red conglomerate, sandstone, and mud shale. Despite their vast difference in geological age, these parent materials are characterized by a "weakly magnetic" nature due to the dominance of quartz and silicate minerals with low primary ferromagnetic mineral content, providing a distinctive baseline for studying pedogenic magnetic enhancement.

3. Materials and Methods

3.1. Sampling

A total of 57 soil sites were sampled across Yunnan Province, with their spatial distribution illustrated in Figure 1b. Sampling sites were positioned within the distribution belts of weakly magnetic clastic formations across the Yunnan Plateau. Soil samples were retrieved following a vertical profiling approach, typically reaching depths of 60–100 cm, with incremental layering at 20 cm intervals. Depending on the degree of pedogenic development at each site, 2–5 samples were collected from each profile, yielding a total of 149 soil samples.

To prevent exogenous magnetic interference, all specimens were collected using wooden tools. Each sample, which weighed about 200 g, was allowed to air dry in a lab setting. For the purpose of measuring mineral magnetic parameters, a portion of each sample was then finely ground in an agate mortar and sieved before being packed into 8 cm^3 non-magnetic cubic boxes. The remaining fine earth fraction was used for bulk geochemical testing (major elements). As laboratory backups, leftover samples were sealed and stored.

3.2. Magnetic Measurements

After air-drying at room temperature, soil samples were gently disaggregated and ground to a fine powder. Volume magnetic susceptibility was measured at low (976 Hz) and high (15,616 Hz) frequencies using an MFK1-FA Multi-function Kappabridge (AGICO, Brno, Czech Republic), yielding κ_{lf} and κ_{hf}, respectively. Mass-specific magnetic susceptibility (χ_{lf} and χ_{hf}) was calculated from volume susceptibility according to $\chi = \kappa/\rho$, where ρ is the bulk density of the sample. The percentage frequency-dependent susceptibility (χ_{fd}) is defined as the difference between low-frequency susceptibility (χ_{lf}) and high-frequency susceptibility (χ_{hf}). In practice, the percentage frequency-dependent susceptibility (χ_{fd}%), calculated according to Equation (1), is more commonly used to characterize this parameter. Anhysteretic remanent magnetization (ARM) was imparted using an LDA5/PAM1 alternating-field demagnetizer (AGICO, Brno, Czech Republic) by applying a decaying alternating magnetic field with a peak amplitude of 100 mT, superimposed with a steady direct bias field of 0.05 mT. After removal of all external fields, the ARM was measured using a JR-6A dual-speed spinner magnetometer (AGICO, Brno, Czech Republic), and the χ_{ARM} was subsequently calculated according to Equation (2), where H denotes the applied direct bias field (0.05 mT). Saturation isothermal remanent magnetization (SIRM)

was measured following the same procedure, with a maximum applied magnetic field of 1 T.

$$\chi_{fd}\% = \frac{\chi_{lf} - \chi_{hf}}{\chi_{lf}} \times 100\% \quad (1)$$

$$\chi_{ARM} = \frac{ARM}{H} \quad (2)$$

3.3. Chemical Analysis

Epsilon 5 High-energy polarized energy-dispersive X-ray fluorescence spectrometry (PANalytical B.V., Almelo, The Netherlands) was used to measure the concentrations of major elements, such as Fe, Al, Si, K, Ca, Mg, Na, and P [32].

3.4. Assessments of Pedogenic Processes

A number of pedogenic indices, such as the silica–alumina ratio (Sa), silica–alumina–iron ratio (Saf), the Chemical Index of Alteration (CIA), and the Chemical Index of Weathering (CIW), were calculated by Equations (3)–(6) based on the obtained major oxide data. Among these indices, CIA was proposed by Nesbitt and Young [24,25], CIW, Sa, and Saf were defined by Harnois [23] and Rocha Filho [33]. In the calculation of CIA and CIW, CaO refers exclusively to calcium derived from silicate minerals. Following the correction method proposed by Roddaz et al. [34], CaO* is defined as CaO when CaO $\leq Na_2O$, whereas CaO* is taken as equal to Na_2O when CaO > Na_2O. These indices were used to describe the degree of chemical weathering and element redistribution during pedogenesis. Specifically, according to the classification criteria defined by Feng et al. [20], CIA values of 50–65 reflect weak weathering, 65–85 represent moderate weathering, and values exceeding 85 indicate strong weathering.

$$CIA = 100 \times \frac{Al_2O_3}{Al_2O_3 + CaO^* + Na_2O + K_2O} \quad (3)$$

$$CIW = 100 \times \frac{Al_2O_3}{Al_2O_3 + Na_2O + CaO^*} \quad (4)$$

$$Sa = \frac{Si_2O_3}{Al_2O_3} \quad (5)$$

$$Saf = \frac{Si_2O_3}{Al_2O_3 + Fe_2O_3} \quad (6)$$

3.5. Data Processes

Statistical evaluation and bivariate correlation analyses for the integrated soil datasets were conducted using Origin 2022 to elucidate inter-parameter relationships and generate fundamental graphical representations. The geospatial distribution of georeferenced sampling sites was characterized and mapped via ArcGIS version 10.7. Unless otherwise specified, the significance of all statistical outputs was rigorously assessed at the 95% confidence level (α = 0.05).

4. Results

4.1. Variations in Magnetic Parameters

This study systematically delineates critical magnetic parameters to analyze the integrated magnetic fingerprints and pedogenically driven spatial heterogeneity in Yunnan soils generated from clastic rock parent materials. Specifically, the results of low-frequency susceptibility (χ_{lf}), frequency-dependent susceptibility (χ_{fd}), percentage frequency-dependent susceptibility (χ_{fd}%), anhysteretic remanent magnetization susceptibility (χ_{ARM}), and sat-

uration isothermal remanent magnetization (SIRM), as well as the χ_{ARM}/χ_{lf} ratio, are summarized in Table 1. Moreover, vertical distribution patterns of ten typical soil profiles in χ_{lf}, χ_{fd}, χ_{fd}%, and χ_{ARM}, measured by conventional methods and calculated based on the measurements, are presented in Figure 2.

Table 1. Magnetic parameters of soil.

Magnetic Parameters	Minimum	Maximum	Mean Value ± Standard Deviation	Coefficient of Variation
χ_{lf} (10^{-8} m^3/kg)	2.543	595.652	109.941 ± 128.035	1.165
χ_{fd} (10^{-8} m^3/kg)	0.137	101.043	15.937 ± 20.202	1.268
χ_{ARM} (10^{-8} m^3/kg)	13.243	2860.853	572.346 ± 607.949	1.062
SIRM (10^{-3} Am^2/kg)	0.285	8.090	2.951 ± 2.313	0.784
χ_{fd}%	5.403	17.574	12.898 ± 3.127	0.242
χ_{ARM}/χ_{lf}	0.956	25.533	5.821 ± 2.773	0.476

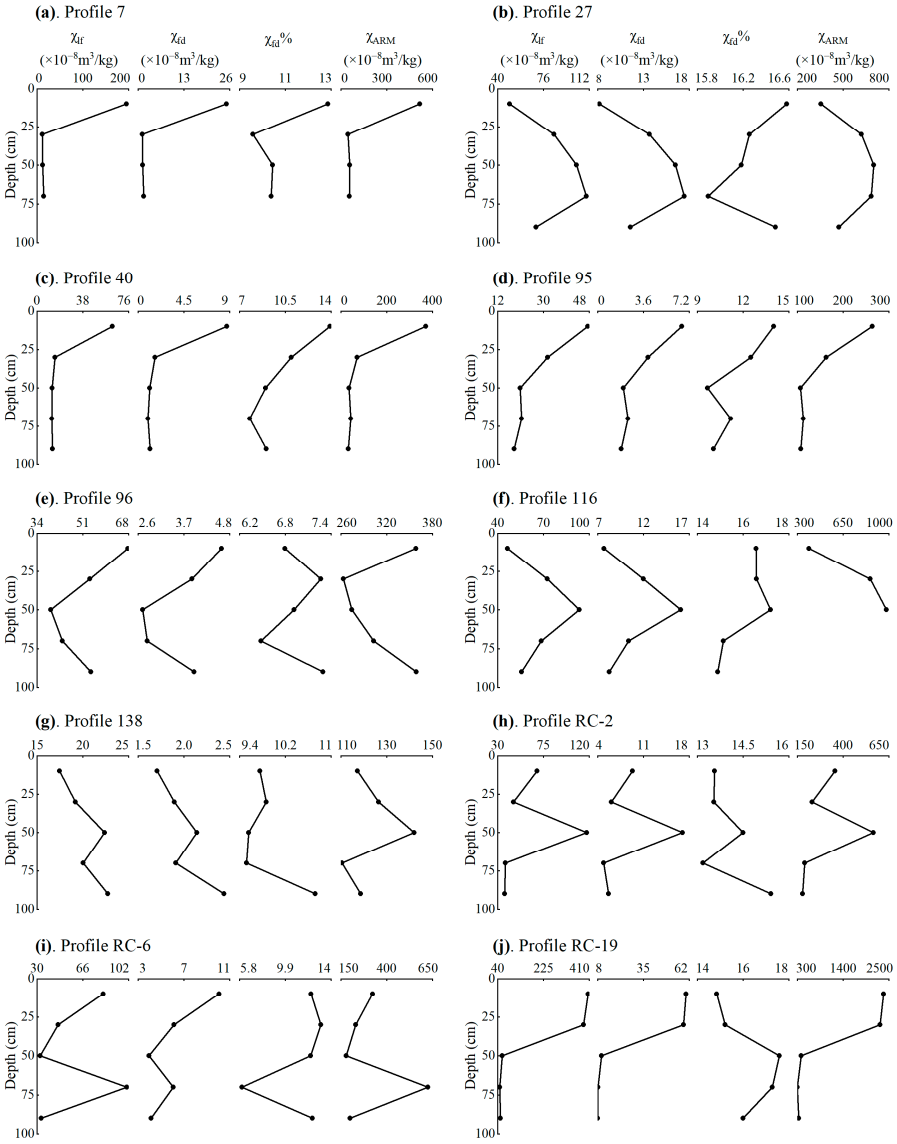


Figure 2. Vertical distributions of magnetic parameters in representative soil profiles. (**a**) Profile 7; (**b**) Profile 27; (**c**) Profile 40; (**d**) Profile 95; (**e**) Profile 96; (**f**) Profile 116; (**g**) Profile 138; (**h**) Profile RC-2; (**i**) Profile RC-6; (**j**) Profile RC-19.

The statistical characterization of soil magnetic parameters provides critical insights into the integrated magnetic intensity and the fundamental mineralogical properties of the soil in the study area [35]. The low-frequency susceptibility (χ_{lf}) measured at the bottom of the soil profiles averages 105.993 $\times$ 10^{-8} m^3/kg, which signifies that the parent materials across the sampling sites are inherently weakly magnetic. As summarized in Table 1, the low-frequency magnetic susceptibility (χ_{lf}) ranges from 2.543 $\times 10^{-8}$ m^3/kg to 595.652 $\times$ 10^{-8} m^3/kg, with a mean value of 109.941 $\times$ 10^{-8} m^3/kg. Upon differentiating by parent rock lithology, the magnetic characteristics of the soil samples exhibit a discernible degree of variability. For soils derived from mudstone/shale, the χ_{lf} ranges from 8.769 $\times$ 10^{-8} m^3/kg to 595.652 $\times$ 10^{-8} m^3/kg, with a mean value of 113.729 $\times$ 10^{-8} m^3/kg. In contrast, sandstone-derived soils show χ_{lf} values between 2.543 and 372.267 $\times$ 10^{-8} m^3/kg, yielding a slightly lower mean of 88.703 $\times$ 10^{-8} m^3/kg. While their distribution ranges overlap, the magnetic intensity of sandstone-derived soils is generally subordinate to that of mudstone/shale-derived profiles. Soils developed on conglomerate exhibit a higher mean χ_{lf} of 244.502 $\times$ 10^{-8} m^3/kg; however, these results are intended primarily for reference due to the limited sample size (four sampling sites), which constrains their broader statistical representativeness.

The degree of coefficient of variation (CV) can be evaluated using the following classification: CV < 0.1 indicates weak variation, 0.1 $\leq$ CV $\leq$ 0.3 indicates moderate variation, and CV > 0.3 indicates strong variation [36]. Across the three clastic lithologies, the coefficient of variation (CV) for χ_{lf} ranges from 0.68 to 1.29, signifying strong variability and reflecting substantial heterogeneity in the concentration and types of magnetic mineral assemblages within the soil matrices. Regarding remanence properties, the saturated isothermal remanent magnetization (SIRM) for sandstone and mudstone/shale-derived soils varies from 0.285 to 8.09 $\times$ 10^{-3} Am^2/kg. This suggests a dominance of ferrimagnetic minerals, though a discernible contribution from high-coercivity hard magnetic minerals is also present in certain samples. Notably, SIRM values for conglomerate-derived soils consistently exceed 1.95 $\times$ 10^{-3} Am^2/kg, indicating a relatively higher proportion of hard magnetic components compared to the other clastic-derived soils.

The percentage frequency-dependent susceptibility (χ_{fd}%), which is the key metric for evaluating the relative contribution of superparamagnetic SP grains, shows a mean value of 12.898% with a maximum value up to 17.574%. Unlike the concentration-dependent parameters, the CV of χ_{fd}% is 0.242, falling within the moderate variation range (0.1 $\leq$ CV $\leq$ 0.3). For sandstone-derived soils, the χ_{fd}% ranges from 5.404% to 20.772%, while mudstone/shale-derived counterparts exhibit values between 5.018% and 17.574%, with a CV of 0.268, suggesting a highly dispersed magnetic grain size distribution, implying that the soil matrices likely harbor a heterogeneous mixture of superparamagnetic (SP) particles and coarser magnetic grains. In contrast, conglomerate-derived soils yield χ_{fd}% values consistently exceeding 10.87%, which signifies that the ferrimagnetic mineral assemblage is predominantly composed of pedogenic SP particles. Furthermore, the variations in χ_{fd} and anhysteretic remanent susceptibility (χ_{ARM}) align closely with the trends observed in χ_{lf} for both sandstone and mudstone/shale-derived soils. This synchronous behavior indicates that mudstone/shale-derived soils generally host a higher concentration of SP and single-domain (SD) magnetic minerals compared to those developed from sandstone. The χ_{ARM}/χ_{lf} ratio exhibits a mean value of 5.821, with a distributional range spanning 0.956 to 25.533. These results detail the quantitative distribution of magnetic concentration and granulometry across the investigated soil profiles.

Figure 2 presents the vertical distribution patterns of key magnetic proxies within representative soil profiles in the studied area. The vertical magnetic characteristics of the clastic-derived soil profiles can be categorized into three primary patterns based on the

distribution of concentration-dependent parameters: (1) Surface enrichment pattern: In this group, concentration-dependent parameters (e.g., χ_{lf}, χ_{fd}, χ_{fd}%, and χ_{ARM}) exhibit pronounced maximum values in the surface or near-surface horizons (e.g., mudstone-derived profiles 7, 40, and 95; sandstone-derived profiles RC-6 and RC-19) and systematically decrease with depth. This indicates a higher concentration of ferrimagnetic minerals in the upper solum. Specifically, values of χ_{fd}% exceeding 10% in the upper 40 cm indicate a preferential enrichment of superparamagnetic (SP) particles in the surface soil [10]. (2) Subsurface peak pattern: Parameters such as χ_{lf}, χ_{fd}, and χ_{ARM} initially increase and then decrease with depth (e.g., conglomerate profile 27, siltstone profile 116, and mudstone profile 138). The magnitude and trends of χ_{fd}% vary significantly in these profiles, suggesting that the magnetic signals are primarily governed by the type and concentration of magnetic minerals rather than grain size distribution. (3) Stochastic fluctuation pattern: These profiles display jagged or sawtooth-like curves, where χ_{lf}, χ_{fd}, χ_{fd}%, and χ_{ARM} fluctuate irregularly with depth (e.g., sandstone profile RC-2). This erratic behavior is likely attributed to the heterogeneous presence of Fe-Mn nodules within the soil matrix.

A comprehensive analysis of the 57 soil profiles reveals that the surface enrichment pattern is the dominant vertical trend. This suggests that the upper soil horizons are characterized by an abundance of ferrimagnetic minerals, primarily within the SP and SD grain size ranges. Conversely, the deeper layers contain a higher proportion of high-coercivity minerals, such as hematite and goethite, with magnetic carriers dominated by SSD and MD (multidomain) particles. These systematic vertical differentiations highlight the concentration of magnetic enhancement in the upper soil horizons compared to the underlying parent material. However, it should be noted that, in the absence of independent chronological constraints, the observed vertical differentiation cannot be unequivocally interpreted as a temporal sequence of soil evolution. Instead, it mainly reflects the relative modification of soil magnetic properties by pedogenic processes under a weakly magnetic clastic parent material background.

4.2. Relationships Among Various Magnetic Parameters

In soils developed on weakly magnetic parent materials, increases in magnetic susceptibility are commonly attributed to the pedogenic neoformation of ferrimagnetic minerals [34]. To further elucidate the intrinsic mechanisms underlying magnetic enhancement in soils developed from weakly magnetic clastic rock parent materials in Yunnan Province and to constrain the grain size and distribution of magnetic minerals, this study systematically examines the relationships among χ_{lf}, χ_{fd}, χ_{fd}%, χ_{ARM}, and SIRM.

As shown in Figure 3a,b, χ_{lf} exhibits an exceptionally strong positive linear correlation with χ_{fd}, with a coefficient of determination (R^2) as high as 0.965, while it presents a considerable non-linear correlation with χ_{fd}% (R^2 = 0.307). Additionally, χ_{lf} shows a significant positive correlation with χ_{ARM} (Figure 3c; R^2 = 0.725), which primarily reflects the existence and increase in the stable single-domain (SSD) particles during the pedogenic process [9]. In contrast, the relationship between χ_{lf} and SIRM is relatively weak, with an R^2 value of 0.212 (Figure 3d).

The parameters χ_{fd} and χ_{fd}% serve as key diagnostic indicators for the presence of ultrafine SP particles (<0.03 μm) in soils [17]. As shown in Figure 3b, the majority of samples display χ_{fd}% values in the range of 8%–17%, indicating that superparamagnetic SP particles dominate the newly formed magnetic mineral assemblage. Notably, χ_{fd}% remains consistently at a high level while χ_{lf} values increase from 2.543×10^{-8} m^3/kg to 595.652×10^{-8} m^3/kg. Furthermore, positive linear relationships are observed between χ_{lf} and χ_{fd}/χ_{ARM} (Figure 3e; R^2 = 0.247), as well as between SIRM and χ_{ARM} (Figure 3f;

R^2 = 0.460). These statistical results detail the coupling between magnetic concentration and grain-size-sensitive parameters across the studied samples.

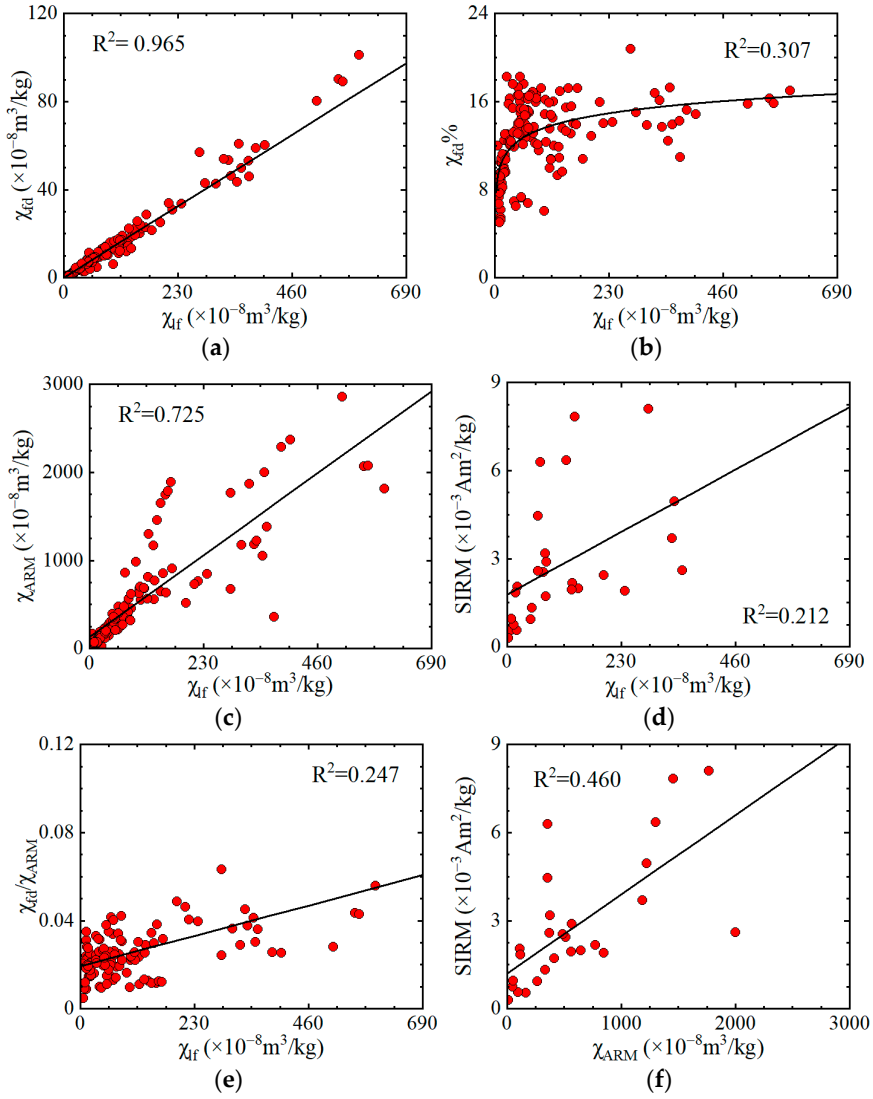


Figure 3. Bivariate plots of relevant magnetic parameters. (**a**) Relationship between low-frequency magnetic susceptibility (χ_{lf}) and frequency-dependent susceptibility (χ_{fd}); (**b**) Relationship between low-frequency magnetic susceptibility (χ_{lf}) and percentage frequency-dependent susceptibility (χ_{fd}%); (**c**) Relationship between low-frequency magnetic susceptibility (χ_{lf}) and anhysteretic remanent magnetization susceptibility (χ_{ARM}); (**d**) Relationship between low-frequency magnetic susceptibility (χ_{lf}) and saturation isothermal remanent magnetization (SIRM); (**e**) Relationship between low-frequency magnetic susceptibility (χ_{lf}) and χ_{fd}/χ_{ARM} ratio; (**f**) Relationship between anhysteretic remanent magnetization susceptibility (χ_{ARM}) and saturation isothermal remanent magnetization (SIRM).

4.3. Bulk Geochemistry Analysis

The bulk geochemistry study provides both a quantitative measure of pedogenic intensity and essential geochemical evidence for evaluating the neoformation of magnetic components throughout soil development [29]. To further examine the pedogenic differentiation of soils developed from weakly magnetic clastic rock parent materials, this study systematically analyzes the vertical distribution patterns of major oxides (SiO_2, Al_2O_3, CaO, and Fe_2O_3) and the Chemical Index of Alteration (CIA) across ten representative soil profiles (Figure 4). In addition, ternary diagrams were constructed to investigate elemental migration pathways and the weathering stage of soil (Figures 5 and 6).

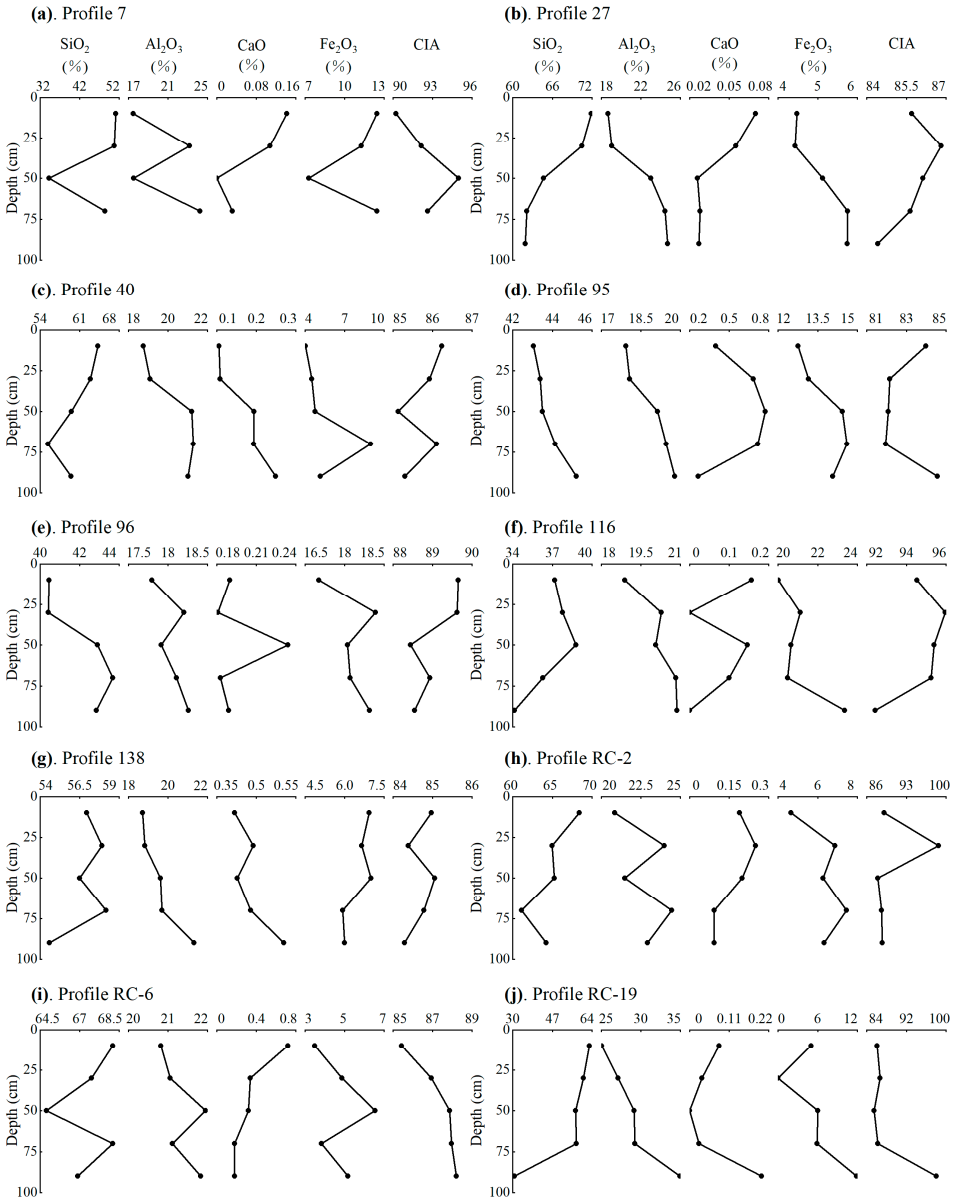


Figure 4. Vertical distributions of major oxides and Chemical Index of Alteration (CIA) in representative soil profiles. (**a**) Profile 7; (**b**) Profile 27; (**c**) Profile 40; (**d**) Profile 95; (**e**) Profile 96; (**f**) Profile 116; (**g**) Profile 138; (**h**) Profile RC-2; (**i**) Profile RC-6; (**j**) Profile RC-19.

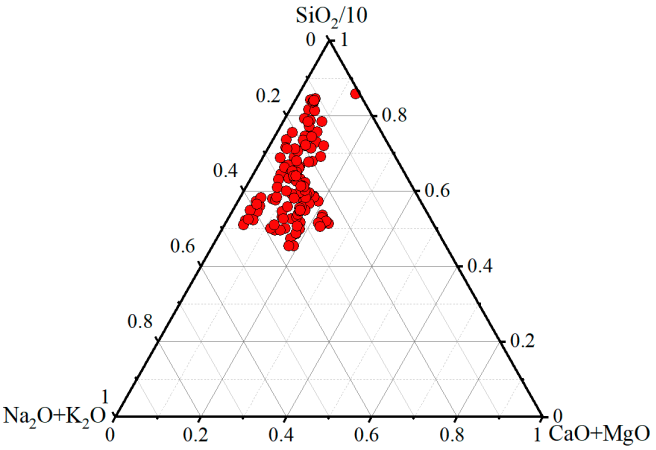


Figure 5. CaO + MgO − $SiO_2/10$ − Na_2O + K_2O ternary diagram.

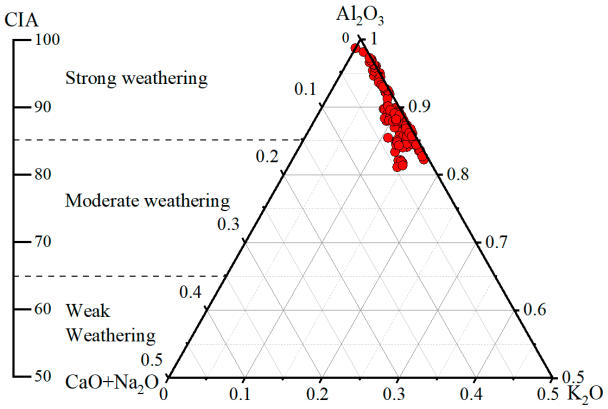


Figure 6. $Al_2O_3 - CaO + Na_2O - K_2O$ (ACNK) ternary diagram.

The vertical distribution patterns of major oxides in the representative soil profiles are shown in Figure 4. In the majority of profiles, SiO_2 contents are relatively higher in surface soils. Influenced by the high concentration of SiO_2, the concentrations of Fe_2O_3 and Al_2O_3 in the surface horizons remain lower than those in the deeper layers. Typically, Fe and Al are incorporated into the formation of secondary clay minerals during weathering, resulting in their relative accumulation in the upper parts of the profile as weathering intensity increases. However, the distribution of Fe_2O_3 and Al_2O_3 in this study presents an inverse trend. This deviation is primarily attributed to the complex high-relief topography of the mountainous Yunnan region. In these non-high-thermal zones, restricted element migration combined with high humidity facilitates the leaching of mobilized Fe and Al from surface minerals, causing them to percolate into the underlying horizons. This vertical geochemical distribution is consistent with the characteristics observed in subtropical soil profiles derived from basaltic and granitic parent materials [37,38].

Alkali and alkaline earth oxides (CaO, Na_2O, MgO, and K_2O) occur at low concentrations throughout the profiles. CaO and Na_2O generally decrease toward the surface, while MgO and K_2O exhibit minor vertical variations. In addition, the Chemical Index of Alteration (CIA) values were calculated to quantify the chemical weathering intensity. The CIA values in the studied soil profiles exhibit certain vertical fluctuations but remain consistently within the range of 80.5 to 99.8, indicating that the soil profiles have undergone moderate-to-strong chemical weathering (according to the classification criteria defined by Feng et al. [20]) under subtropical humid–thermal conditions. However, the CIA exhibits a decreasing trend in the upper horizons, representing an anomaly in weathering intensity. This phenomenon may be attributed to the following factors: (1) Under intense humid-heat weathering, the rapid neoformation of secondary minerals, such as kaolinite, facilitates the swift release and depletion of Ca^{2+}, Na^+, and K^+ ions [39]. (2) Rainfall in the mountainous regions of Yunnan is dominated by localized heavy storms, which can lead to the physical stripping and erosion of the uppermost soil layers, thereby reducing the observable concentrations of Fe and Al oxides at the surface [40]. (3) In high-humidity zones, persistent precipitation drives the downward percolation of soil water, leaching Fe and Al oxides from the upper horizons and promoting their accumulation in the lower profile, which consequently elevates the oxide values in deeper layers [38].

The ternary diagrams of major oxides shown in Figures 5 and 6 further illustrate the overall weathering trends and mineralogical evolution of soils in the study area. As illustrated in Figure 5, soil samples from the research region exhibit a pronounced clustering pattern in the $CaO + MgO - SiO_2/10 - Na_2O + K_2O$ ternary diagram. All data points are markedly displaced away from the CaO + MgO apex and are mainly distributed within the interior region bounded by the $SiO_2/10$ and $Na_2O + K_2O$ end members. This distribution

pattern quantitatively reflects the systematic and rapid leaching of alkaline earth metals (e.g., CaO and Mg) throughout the pedogenic process [41].

In the $Al_2O_3 - CaO + Na_2O - K_2O$ (ACNK) ternary diagram (Figure 6), the weathering trend of soils in the study area is further suggested. Samples are generally aligned along the A−K line toward the Al_2O_3 apex and are positioned far from the K_2O end-member, indicating that the weathering of albite in the soils has been largely completed, and the system has entered a stage characterized by progressive potassium depletion and relative aluminum enrichment. Moreover, the CIA values for the majority of these samples fluctuate vertically across the profiles but remain consistently within the range of 80.5 to 99.8.

4.4. Correlation Between Magnetic Parameters and Pedogenic Indices

To quantitatively reveal the response of magnetic enhancement to pedogenic processes in soils developed from weakly magnetic clastic rock parent materials, this study systematically examines the quantitative relationships between magnetic parameters (e.g., χ_{lf}, χ_{fd}, χ_{fd}%, χ_{ARM}, and SIRM), their derived ratios, and pedogenic indicators (e.g., CIA, CIW, Sa, and Saf). Meanwhile, bivariate plots of magnetic parameters and pedogenic indices exhibiting strong correlations are presented in Figure 7 to visually illustrate the relationships between these variables.

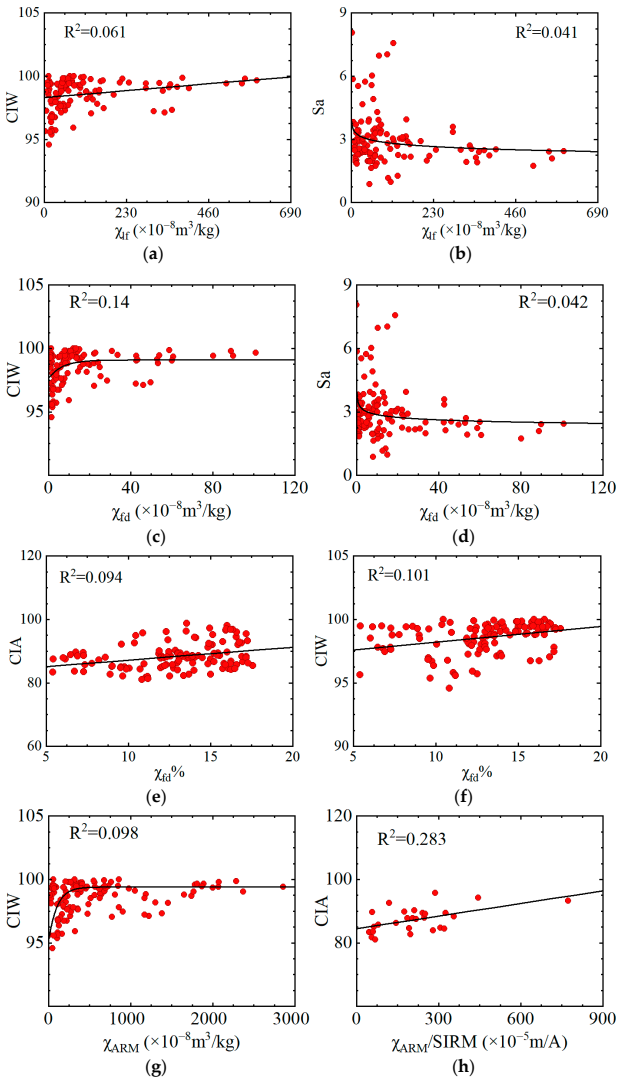


Figure 7. Bivariate plots of magnetic parameters and pedogenic indices. (**a**) Relationship between low-frequency magnetic susceptibility (χ_{lf}) and chemical index of weathering (CIW); (**b**) Relationship

between low-frequency magnetic susceptibility (χ_{lf}) and silica–alumina ratio (Sa); (**c**) Relationship between frequency-dependent susceptibility (χ_{fd}) and chemical index of weathering (CIW); (**d**) Relationship between frequency-dependent susceptibility (χ_{fd}) and silica–alumina ratio (Sa); (**e**) Relationship between percentage frequency-dependent susceptibility (χ_{fd}%) and chemical index of alteration (CIA); (**f**) Relationship between percentage frequency-dependent susceptibility (χ_{fd}%) and chemical index of weathering (CIW); (**g**) Relationship between anhysteretic remanent magnetization susceptibility (χ_{ARM}) and chemical index of weathering (CIW); (**h**) Relationship between χ_{ARM}/SIRM ratio and chemical index of alteration (CIA).

The Pearson correlation analysis between magnetic parameters and pedogenic indices is summarized in Table 2. Statistically significant correlations at the 95% confidence level ($p < 0.05$) are indicated by an asterisk (*). Statistical results demonstrate that while certain soil magnetic parameters are significantly correlated with pedogenic indices, others exhibit relatively weak correlations. This disparity is primarily attributed to the anomalous vertical geochemical distribution characteristic of soil profiles in humid–thermal regions. Such correlations indicate that an intrinsic link persists between soil magnetism and pedogenic processes, even though underlying environmental complexities may attenuate the overall correlation strength. Specifically, χ_{lf} exhibits a significant positive correlation with the chemical weathering index (CIW, r = 0.24, $p < 0.05$), whereas its linear regression with the Chemical Index of Alteration (CIA) shows only a weak positive trend with a low r of 0.09. Additionally, χ_{lf} displays a significant negative correlation with the silica–alumina ratio (Sa, r = −0.18, $p < 0.05$), and the corresponding bivariate plot (Figure 7b) exhibits a pronounced non-linear decreasing trend with a coefficient of determination of 0.041. These statistical values indicate that magnetic parameters exhibit significant correlations with pedogenic indices, indicating a close coupling between soil magnetic properties and pedogenic processes.

Table 2. Pearson correlation analysis results of magnetic parameters and pedogenic indices.

Parameters	χ_{lf}	χ_{fd}	χ_{fd}%	χ_{ARM}	SIRM	χ_{ARM}/SIRM	χ_{ARM}/χ_{lf}	χ_{fd}/χ_{ARM}	CIA	CIW	Sa
χ_{lf}	1.00										
χ_{fd}	0.98 *	1.00									
χ_{fd}%	0.27 *	0.37 *	1.00								
χ_{ARM}	0.85 *	0.85 *	0.46 *	1.00							
SIRM	0.46 *	0.40 *	0.18	0.68 *	1.00						
χ_{ARM}/SIRM	0.67 *	0.72 *	0.64 *	0.64 *	−0.05	1.00					
χ_{ARM}/χ_{lf}	−0.18 *	−0.18 *	0.05	0.16	0.01	0.05	1.00				
χ_{fd}/χ_{ARM}	0.43 *	0.43 *	0.35 *	0.07	−0.04	0.40 *	−0.55 *	1.00			
CIA	0.09	0.09	0.30 *	0.15	0.14	0.53 *	−0.08	0.14	1.00		
CIW	0.24 *	0.26 *	0.31 *	0.27 *	0.14	0.40 *	−0.05	0.16	0.55 *	1.00	
Sa	−0.18 *	−0.18 *	−0.10	−0.17	−0.28	−0.39 *	0.08	−0.10	−0.29 *	−0.19 *	1.00
Saf	−0.17	−0.16	−0.07	−0.16	−0.27	−0.39 *	0.07	−0.08	−0.33 *	−0.14	0.96 *

* ($p < 0.05$).

The correlations between grain-size-sensitive magnetic parameters (χ_{fd}% and χ_{ARM}/SIRM) and geochemical pedogenic indices are presented in Table 2. Specifically, χ_{fd}% is positively correlated with both the CIA (r = 0.30, $p < 0.05$) and the CIW (r = 0.31, $p < 0.05$). In addition, χ_{ARM}/SIRM displays a positive correlation with CIA (r = 0.53, $p < 0.05$). The relationships among these parameters, along with the correlations between χ_{lf} and the silica–alumina ratio (Sa), characterize the linear associations between magnetic grain size indicators and chemical weathering degrees across the studied soil profiles.

5. Discussion

5.1. Magnetic Properties of Weakly Magnetic Clastic Rock

This study systematically investigates the magnetic properties of soils developed on weakly magnetic clastic rock parent materials in Yunnan Province and demonstrates that, under a distinctive low magnetic background, the neoformation of fine-grained pedogenic magnetic minerals during soil development leads to a pronounced enhancement of soil magnetic signals. The relatively low mean low-frequency susceptibility (χ_{lf}) of the investigated soils (109.941×10^{-8} m^3/kg), together with the similarly low χ_{lf} values observed at the bottom of the soil profiles (105.993×10^{-8} m^3/kg) compared with those reported for soils derived from strongly magnetic parent materials [42], confirms the weak magnetic baseline of the study area. This difference mainly reflects the intrinsically low abundance of primary ferrimagnetic minerals in sedimentary clastic parent rocks. Statistical results further show that, for soils derived from both sandstone and mudstone/shale, the coefficients of variation (CV) of low-frequency susceptibility (χ_{lf}) and SIRM are close to 1, indicating strong spatial variability in magnetic intensity. Such variability suggests that, although the parent material provides the fundamental magnetic background, the magnitude and distribution of magnetic signals are predominantly controlled by pedogenic processes rather than simple inheritance from the parent rocks. The vertical profiles of χ_{lf} generally display a marked decrease from surface horizons toward the parent material. This pronounced top-down attenuation implies that the enhanced magnetic signal in surface soils is mainly associated with pedogenic processes during soil formation, while the contribution of inherited magnetic minerals is relatively limited [15]. Furthermore, the frequency-dependent susceptibility (χ_{fd}%) exhibits a wide range (5.403%–17.574%) with a relatively high mean value (12.898%), indicating that most samples contain abundant superparamagnetic (SP) grains. These ultrafine magnetic particles are likely formed through pedogenic weathering and soil-forming processes, reflecting the in situ transformation and neoformation of ferrimagnetic minerals under dynamic soil environmental conditions.

To further illustrate the SP content and weathering strength and to decipher the magnetic grain size and the relative contribution of SP grains, the bivariate plot of χ_{lf} and $\chi_{fd\text{-}B}$% and the Dearing plot were constructed, where $\chi_{fd\text{-}B}$% represents the percentage frequency-dependent susceptibility equivalent to that measured using Bartington instruments. It should be noted that the low-frequency and high-frequency magnetic susceptibilities reported in this study were measured using an MFK1-FA Multi-function Kappabridge at excitation frequencies of 976 Hz and 15,616 Hz, respectively. In Figures 8 and 9, the χ_{fd} obtained from the MFK1-FA instrument was recalculated by the following Equation (7) proposed by Hrouda [43] to normalize the results to the frequency ratio of 1:10 commonly employed by Bartington instruments, where $\chi_{fd\text{-}B}$ represents the percentage frequency-dependent susceptibility equivalent to that measured using Bartington instruments, χ_{fd} is the frequency-dependent susceptibility measured by the MFK1-FA instrument, and f_{mHF} and f_{mLF} correspond to the high (15,616 Hz) and low (976 Hz) operating frequencies of the MFK1-FA system, respectively. This conversion allows for a more consistent evaluation of SP particle contributions and facilitates comparison with previously published datasets.

$$\chi_{fd\text{-}B} = \frac{\ln 10}{\ln f_{mHF} - \ln f_{mLF}} \chi_{fd} \quad (7)$$

As shown in Figure 8, the bivariate plot of χ_{lf} and $\chi_{fd\text{-}B}$% further highlights the components of fine grains (particularly SP particles) and coarser grains in the newly formed magnetic minerals. Specifically, the recalculated $\chi_{fd\text{-}B}$% is mainly in the range of 3%–14% with a majority value between 6%–10%, indicating that most of the samples containing magnetic minerals consist of a mixture of SP and coarser grains, part of the samples consist

of only SP grains, while no sample consists of all coarser grains. It is worth noting that the majority of samples display $\chi_{fd\text{-}B}$% values more than 7%, indicating that superparamagnetic SP particles dominate the newly formed magnetic mineral assemblage. Additionally, χ_{fd}% exhibits a strong non-linear relationship with low-frequency susceptibility χ_{lf} (Figure 3b; R^2 = 0.307), suggesting the pedogenic process on the Yunnan Plateau has reached a kinetic equilibrium, yielding a consistent magnetic grain size assembly. This phenomenon aligns with the findings of Ouallali [44], who noted that under stable humid/subtropical conditions, the neoformation of ferrimagnets follows a specific crystallization pathway, producing a relatively constant ratio of SP to SSD grains. Furthermore, the non-linear relationship between concentration and grain size indicators has been interpreted as a saturation of the pedogenic process [45]. Once the pedogenic iron oxide pool is established, further weathering increases the total concentration (χ_{lf}) but does not significantly shift the particle size distribution, as the crystallization kinetics are governed by the regional environmental template rather than the absolute iron availability. This high degree of χ_{fd}% under a wide range of χ_{lf} indicates that, under the warm and humid pedogenic conditions of the Yunnan Plateau, the initial weathering of clastic parent materials is characterized by the rapid accumulation of ultrafine magnetic minerals (e.g., maghemite). As weathering progresses, the relative distribution of magnetic grain sizes reaches a steady state, and the overall magnetic signal is primarily determined by the mineralogical transition between different ferrimagnetic species.

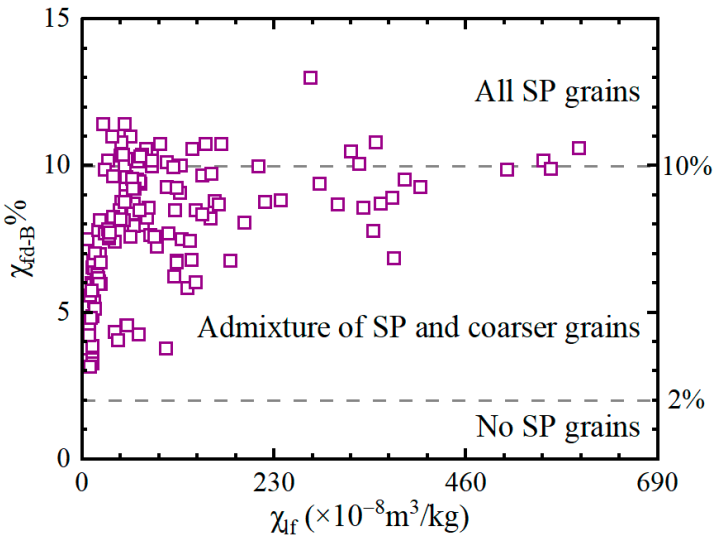


Figure 8. Relationship between χ_{lf} and $\chi_{fd\text{-}B}$% for determining SP content and weathering strength.

This relationship provides compelling evidence that the increase in total magnetic susceptibility is overwhelmingly controlled by the neoformation of nanoscale superparamagnetic SP particles during pedogenesis. In contrast, the weak correlation between χ_{lf} and SIRM (R^2 = 0.212) suggests that the contribution of coarse-grained magnetic minerals inherited from the parent material is relatively limited [15,29].

As shown in Figure 9, a Dearing plot (χ_{ARM}/SIRM vs. $\chi_{fd\text{-}B}$%) was constructed to characterize the magnetic properties of surface soil samples, which shows that the majority of samples cluster within the SD/SP transition zone. This distribution pattern, presented in Figure 9, indicates that the soil magnetic assemblage in the study area is dominated by fine-grained minerals formed through pedogenic processes. It also implies a limited contribution from exogenous inputs, such as industrial fly ash, which is typically characterized by coarse-grained multidomain (MD) particles with low $\chi_{fd\text{-}B}$% values [46]. Considering the contour lines of the Dearing plot, the majority of samples exhibit SP

contributions exceeding 50% of the total magnetic signal, with some approaching 75%, whereas the contribution from MD particles remains negligible. These further rule out any substantial influence of externally derived coarse-grained magnetic materials. Meanwhile, the significant positive correlation between χ_{ARM} and SIRM ($R^2 = 0.460$) suggests that stable single-domain (SSD) particles, acting as the principal carriers of remanent magnetization, maintain good stability throughout the pedogenic process [10]. In combination with the extremely low mean χ_{ARM}/χ_{lf} ratio (5.821) and the characteristics of related ratio parameters, the dominant magnetic carriers in the study area are inferred to be magnetite or maghemite [3,14]. Moreover, the weak upward trend observed between χ_{fd}/χ_{ARM} and χ_{lf} (Figure 3e; $R^2 = 0.247$) may record a dynamic growth pathway during pedogenesis, reflecting the gradual transformation of SP particles into the SSD size range and highlighting the continuity of iron oxide crystal development under progressive soil formation.

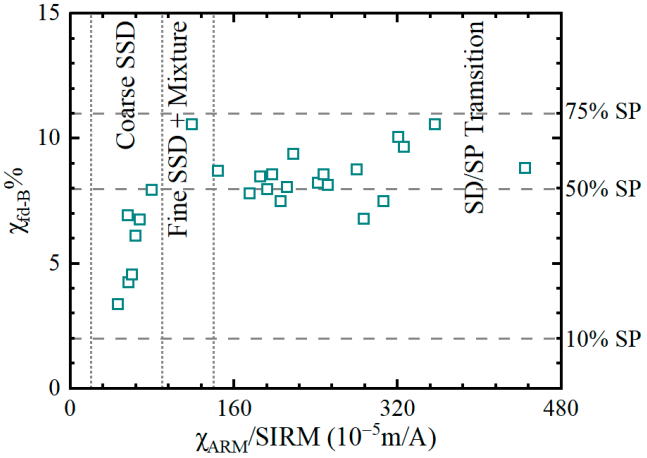


Figure 9. Dearing plot for the samples to decipher the magnetic grain size and the relative contribution of SP grains. The horizontal dashed lines represent the relative contribution of superparamagnetic (SP) grains to the total magnetic susceptibility, corresponding to 10%, 50%, and 75% SP contributions. The vertical dotted lines indicate reference grain-size boundaries of magnetic minerals based on published study [2], corresponding to χ_{ARM}/SIRM values of 20×10^{-5} m/A, 90×10^{-5} m/A, and 140×10^{-5} m/A from left to right, respectively.

Overall, the soil magnetic system in the study area exhibits a characteristic pattern of pronounced pedogenic enhancement superimposed on a weakly magnetic parent material background. The underlying mechanism of magnetic enhancement is primarily governed by the coupled neoformation and accumulation of superparamagnetic SP and fine-grained stable single-domain (SSD) particles; this pattern is fully consistent with the geochemical evidence. The magnetic characteristics of soils developed on weakly magnetic clastic rock parent materials are closely coupled with the elemental variation processes revealed by geochemical analyses. As the CIA increases progressively upward and reaches maximum values in the surface horizons (generally between 80 and 100), the soils undergo intensive elemental reorganization, characterized by substantial leaching of alkali metals (e.g., Na, K) and alkaline earth metals (e.g., CaO and MgO) as well as silica, accompanied by residual enrichment of Fe and Al components [29]. This geochemical transition not only provides an abundant iron source for the formation of secondary magnetic minerals (e.g., maghemite) but also explains the synchronous enhancement of SP and SSD particles in surface soils. Notably, as shown in Table 1, the coefficient of variation of χ_{fd}% (0.242) is markedly lower than that of χ_{lf} (1.165), indicating a clear contrast between the relative stability of grain-size-sensitive parameters and the strong spatial variability of bulk magnetic susceptibility. This pattern suggests that, although the absolute concentration of magnetic minerals varies among sites in response to local microenvironmental differences, the efficiency of

pedogenetic processes in producing fine-grained magnetic minerals remains comparatively uniform across the clastic rocks of the Yunnan Plateau.

Consequently, magnetic parameters sensitive to fine particles, such as χ_{fd}% and χ_{ARM}/SIRM, provide more stable and reliable indicators of regional pedogenic intensity and chemical weathering within the weakly magnetic clastic rock systems investigated in this study. Despite the strong correlations observed in this study, the use of magnetic grain size parameters such as χ_{fd}% and χ_{ARM}/SIRM as quantitative proxies for chemical weathering remains debated. Existing studies [47,48] have shown that these parameters may also be influenced by lithogenic contributions, sedimentary sorting, and post-depositional alteration, which can obscure pedogenic signals in certain geological settings. In particular, the inheritance of primary ferrimagnetic minerals from parent materials may weaken the sensitivity of magnetic proxies to weathering intensity. Therefore, their broader applicability to other lithological and climatic contexts requires further validation.

5.2. Relationships Between Magnetic Parameters and Pedogenic Indices

The combined evidence from correlation analyses (Table 2), bivariate plots (Figure 7), and bulk geochemistry analysis indicates a strong and internally consistent coupling between soil magnetic properties and pedogenic intensity in soils developed on weakly magnetic clastic rock parent materials. In the Yunnan Plateau, where the lithogenic magnetic background is inherently low, soil magnetic signals are particularly sensitive to pedogenic modification and thus provide a high-resolution archive of weathering-driven mineral transformations.

Figure 10 presents a correlation heatmap to more visually illustrate the relationships between major magnetic parameters and pedogenic indices in the study area. Overall, the results indicate that soil magnetic properties are closely linked to pedogenic intensity under the weakly magnetic clastic rock parent material background. Parameters indicative of fine-grained magnetic mineral abundance (χ_{fd}% and χ_{ARM}) exhibit more significant positive correlations with the Chemical Index of Weathering (CIW) than χ_{lf}. This contrast indicates that, under a weakly magnetic background, variations in magnetic grain size distribution respond more sensitively to pedogenic processes than changes in the absolute concentration of magnetic minerals, which may be partially influenced by minor lithological heterogeneity. Mechanistically, this response reflects the progressive breakdown of primary silicate minerals during weathering, coupled with the residual enrichment of Fe and Al elements [29].

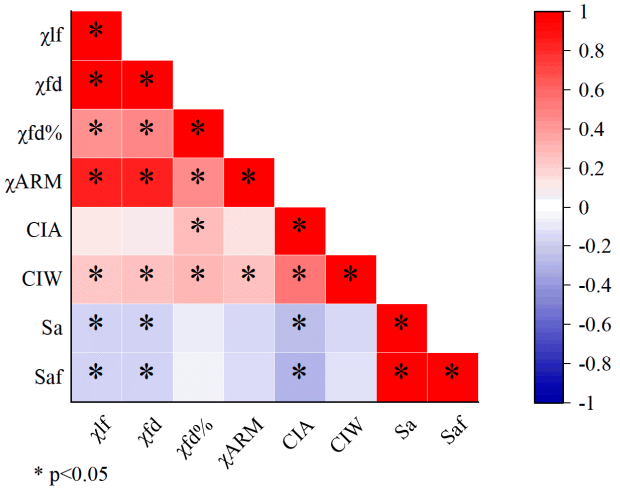


Figure 10. Heatmap of main magnetic parameters and pedogenic indices.

Additionally, the linkage between soil magnetic enhancement and chemical weathering can be further clarified by bulk geochemical evidence. As shown in the ACNK ternary diagram (Figure 6) in Section 4.3, most samples plot along the A-K trend toward the Al_2O_3 apex, with approximately 78% of the investigated soil profiles having reached the stage of strong weathering (CIA > 85), while only 22% fall into the category of moderate weathering (CIA: 65–85), which may indicate an advanced stage of pedogenesis marked by extensive breakdown of plagioclase and other primary silicate minerals [41]. Iron is gradually released from silicate crystal lattices as a result of such severe weathering. Repeated wetting-drying cycles help mobilize and redistribute iron under the warm, humid climate of the Yunnan Plateau, enabling it to undergo oxidation and reprecipitation as secondary ferrimagnetic phases. Superparamagnetic SP and stable single-domain (SSD) particles, most likely in the form of maghemite, predominate in the formation of fine-grained pedogenic magnetic minerals. The remarkably strong positive correlation between χ_{ARM}/SIRM and CIA (r = 0.53), which shows that magnetic grain size fining closely tracks the development of chemical weathering, supports this interpretation. On the other hand, the silica–alumina ratio (Sa) and the silica–alumina–iron ratio (Saf) exhibit consistently significant negative correlations with χ_{lf} and χ_{ARM}. Geochemically speaking, these relationships show a weathering regime dominated by desilication under severe leaching conditions, where Fe and Al accumulate residually within the soil system, and SiO_2 is preferentially removed by runoff [29].

The surface enhancement of magnetic parameters corresponds closely to the vertical geochemical patterns observed in representative soil profiles (Figure 4). Under the weakly magnetic background of sedimentary clastic parent materials, pedogenic processes promote the redistribution of iron within the soil profile, particularly through leaching and downward migration under humid subtropical conditions. This redistribution creates favorable conditions for the in situ formation of fine-grained ferrimagnetic minerals in the upper horizons. The consistency between magnetic enhancement and geochemical differentiation suggests that pedogenic modification of iron-bearing phases, rather than simple inheritance from the parent material, plays a dominant role in controlling soil magnetism in these weakly magnetic sedimentary environments.

However, an increasing number of studies have emphasized that parent material can exert a strong control on soil magnetic properties, especially in regions characterized by heterogeneous lithology [49]. In such cases, lithogenic magnetic minerals may significantly contribute to the bulk magnetic signal, leading to potential overestimation of pedogenic enhancement. This issue is particularly important in tropical and subtropical environments, where diverse parent materials may produce variable baseline magnetic backgrounds. In contrast, the weakly magnetic clastic parent materials in the present study provide a favorable condition for isolating pedogenic magnetic signals from lithogenic background contributions. Because the primary ferrimagnetic mineral content of the parent material is relatively low, the bulk magnetic susceptibility is less dominated by inherited lithogenic components. This setting enhances the detectability of pedogenically formed fine-grained ferrimagnetic particles, thereby improving the sensitivity of grain-size-dependent parameters such as χ_{fd}% and χ_{ARM}/SIRM to variations in chemical weathering intensity. It should be noted that this advantage is context-specific. In regions where parent materials contain abundant primary magnetite or other ferrimagnetic minerals, lithogenic signals may mask or dilute pedogenic enhancement, potentially weakening the reliability of magnetic proxies. Therefore, the effectiveness of magnetic parameters as indicators of pedogenesis is closely linked to the magnetic background of the source material and should be evaluated within each geological setting rather than generalized universally.

6. Conclusions

This study integrates environmental magnetic and geochemical analyses to systematically investigate soils developed on weakly magnetic clastic rock parent materials in Yunnan Province, revealing the dominant influence of pedogenic processes on soil magnetic characteristics under a low magnetic background setting. The results demonstrate that, despite the extremely low initial magnetic susceptibility of the clastic rock parent materials, active pedogenic processes promote a systematic enhancement of magnetic signals in surface soils. The exceptionally strong linear correlation between low-frequency susceptibility (χ_{lf}) and frequency-dependent susceptibility (χ_{fd}) indicates that pedogenically formed superparamagnetic SP particles are the primary contributors to soil magnetic enhancement. From a geochemical perspective, this magnetic enhancement is closely synchronized with iron redistribution during chemical weathering. Under weakly magnetic background conditions, conventional magnetic concentration parameters are strongly influenced by parent material heterogeneity, whereas grain-size-sensitive parameters reflecting fine-particle proportions, such as χ_{fd}% and χ_{ARM}/SIRM, exhibit remarkable stability. Their positive correlations with the Chemical Index of Alteration (CIA) support their reliability as quantitative proxies for assessing chemical weathering intensity under weakly magnetic clastic parent materials in the Yunnan subtropical monsoonal region. Their applicability to other geological and climatic settings should be considered provisional, pending further comparative studies. These findings not only refine the theoretical framework of environmental magnetism in subtropical regions with weakly magnetic parent materials but also provide robust support for the high-resolution reconstruction of paleoenvironmental evolution in this region using soil magnetic approaches.

It should be noted that these findings are primarily representative of the weakly magnetic clastic rock backgrounds of the Yunnan Plateau. The spatial heterogeneity of soil development and the lack of high-resolution chronological control remain inherent challenges in precisely quantifying absolute mineral transformation rates. Future studies across a wider range of lithological and climatic settings, combined with the application of absolute dating techniques, will be necessary to further evaluate the general applicability of the proposed magnetic–weathering relationships. In addition, the integration of advanced micro- and nanoscale analytical approaches [50,51] may provide more direct mineralogical evidence for the pedogenic magnetic phases inferred in this study.

Author Contributions: Conceptualization, X.H. and X.Z.; methodology, X.H.; investigation, M.W., H.L. (Haixia Li), S.L., J.W. and G.Y.; data curation, X.H., M.W. and X.Z.; formal analysis, X.H.; writing—original draft preparation, X.H., M.W., X.Z. and H.L. (Haixia Li); writing—review and editing, X.H., M.W., X.Z., H.L. (Haixia Li), S.L., H.L. (Hongzhan Liu); visualization, X.H.; supervision, H.L. (Hongzhan Liu) and H.L. (Haixia Li); project administration, X.Z. and H.L. (Haixia Li). All authors have read and agreed to the published version of the manuscript.

Funding: This research was funded by Yunnan Fundamental Research Projects (grant NO. 202501AS070153, grant NO. 202301AS070087) and supported by the National Natural Science Foundation of China (grant NO. 42064005).

Data Availability Statement: The datasets presented in this article are not readily available because the datasets used and/or analyzed during the current study are available from the corresponding author on reasonable request.

Conflicts of Interest: Xinglin Huang is an employee of Yunnan Celex Technology Co., Ltd. Hongzhan Liu is an employee of Yunnan Geology and Mining Engineering Survey Group Co., Ltd. The authors declare that they have no known competing financial interests or personal relationships that could have appeared to influence the work reported in this paper.

References

1. Amundson, R.; Berhe, A.A.; Hopmans, J.W.; Olson, C.; Sztein, A.E.; Sparks, D.L. Soil and human security in the 21st century. *Science* **2015**, *348*, 1261071. [CrossRef]
2. Amrutha, K.; Warrier, A.K.; Sandeep, K.; Jyothinath, A.; Ananthapadmanabha, A.L.; Shankar, R. Environmental Magnetic Properties of Lateritic Soils from Southwestern India. *Eurasian Soil Sci.* **2021**, *54*, 238–248. [CrossRef]
3. Pulley, S.; Collins, A.L.; Van Der Waal, B. Variability in the Mineral Magnetic Properties of Soils and Sediments within a Single Field in the Cape Fold Mountains, South Africa: Implications for Sediment Source Tracing. *Catena* **2018**, *163*, 172–183. [CrossRef]
4. Han, G.Z.; Zhang, G.L. Changes in Magnetic Properties and Their Pedogenetic Implications for Paddy Soil Chronosequences from Different Parent Materials in South China. *Eur. J. Soil Sci.* **2013**, *64*, 435–444. [CrossRef]
5. Grison, H.; Janovský, M.P.; Lisá, L.; Hasil, J.; Štefan, I.; Hron, K.; Hejcman, M. Magnetic and Geochemical Record of Soil Impacted by 300 Years of Early Medieval Settlement. *Catena* **2023**, *231*, 107368. [CrossRef]
6. Bondar, K.M.; Bakhmutov, V.; Poliachenko, I.; Hlavatskyi, D.; Menshov, O. Magnetic and Chemical Signals of Post-Blast Residue in Soil: A Case Study from Northern Ukraine. *Sci. Total Environ.* **2025**, *977*, 179342. [CrossRef]
7. Liu, Z.; Guo, X.; Liu, X.; Marković, S.B. Comparative Analysis of the Magnetism between Chinese and Serbian Loess Deposits. *Catena* **2022**, *218*, 106569. [CrossRef]
8. Azizi, K.; Zhao, S.; Ayoubi, S.; Kamangarpour, A.; Nabiollahi, K.; Ge, Y.; Zhao, K.; Rodrigo-Comino, J.; Demattê, J.A.M. Integrating Proximal Sensing Data (Soil Spectra and Magnetic Susceptibility) with the Common Covariates to Predict Soil Carbon Pools in Semiarid Regions. *Soil Tillage Res.* **2026**, *256*, 106840. [CrossRef]
9. Long, X.Y.; Ji, J.F.; Balsam, W.; Barrón, V.; Torrent, J. Grain Growth and Transformation of Pedogenic Magnetic Particles in Red Ferralsols. *Geophys. Res. Lett.* **2015**, *42*, 5762–5770. [CrossRef]
10. Lian, Y.C.; Liu, X.M.; Tabrez, A.R.; Mao, X.G.; Ma, M.M.; Qi, X.Y.; Zhou, S.F. The Magnetic Properties of Attock Loess and Its Environmental Significance in Pakistan. *Quat. Int.* **2022**, *616*, 120–132. [CrossRef]
11. Alekseev, A.O.; Shary, P.A.; Malyshev, V.V. Magnetic Susceptibility of Soils as an Ambiguous Climate Proxy for Paleoclimate Reconstructions. *Quat. Int.* **2023**, *661*, 10–21. [CrossRef]
12. Lourenço, A.M.; Sequeira, E.; Sant'Ovaia, H.; Gomes, C.R. Magnetic, Geochemical and Pedological Characterisation of Soil Profiles from Different Environments and Geological Backgrounds near Coimbra, Portugal. *Geoderma* **2014**, *213*, 408–418. [CrossRef]
13. Fattakhova, L.A.; Shcherbakov, V.P.; Kuzina, D.M.; Dautov, A.N.; Sycheva, N.K. Changes in the Magnetic Properties of Soddy-Podzolic Soils Depending on the Conditions of Soil Formation. *Izv. Atmos. Ocean. Phys.* **2020**, *56*, 1235–1246. [CrossRef]
14. Zhao, W.J.; Wang, H.Y.; Zhang, Z.Y.; Feng, S.W.; Zheng, Y.K.; Li, S.; Luo, Y.; Liu, H.Y. Discrimination of Soil Magnetism Enhanced by Land Use and Its Implications for Inferring Alterations in Sediment Sources and Soil Erosion in a Homogeneous Watershed: An Example from the Guizhou Plateau, SW China. *Catena* **2022**, *217*, 106476. [CrossRef]
15. Yang, J.H.; Xia, D.S.; Chen, Z.X.; Wang, S.Y.; Gao, F.Y.; Liu, X.; Zhao, S.; Zhao, L.; Liu, Y. Differentiating Detrital and Pedogenic Contributions to the Magnetic Properties of Aeolian Deposits in the Southern Tibetan Plateau: Implications for Paleoclimatic Reconstruction. *Catena* **2023**, *220*, 106736. [CrossRef]
16. Cervi, E.C.; Maher, B.; Poliseli, P.C.; De Souza, I.G., Jr.; Da Costa, A.C.S. Magnetic Susceptibility as a Pedogenic Proxy for Grouping of Geochemical Transects in Landscapes. *J. Appl. Geophys.* **2019**, *169*, 109–117. [CrossRef]
17. Dos Santos, L.A.C.; De Araújo Pedron, F.; De Souza, V.S., Jr.; Silva, L.S.; Campos, M.C.C.; Araujo, J.K.S. Magnetic and Spectral Signature of Anthropogenic and Non-Anthropogenic Soils to Identify Pedogenetic Processes in Amazonia, Brazil. *Geoderma Reg.* **2023**, *32*, e00622. [CrossRef]
18. Grison, H.; Petrovsky, E.; Hanzlikova, H. Assessing Anthropogenic Contribution in Highly Magnetic Forest Soils Developed on Basalts Using Magnetic Susceptibility and Concentration of Elements. *Catena* **2021**, *206*, 105480. [CrossRef]
19. Kurgaeva, A.; Sedov, S.; Moreno-Roso, S.; Barceinas Cruz, H.; Ortega Guerrero, B.; Solleiro-Rebolledo, E.; Sinitsyn, A. Magnetic Properties as Indicators of Pedogenic and Pyrogenic Processes at the Upper Paleolithic Site of Kostenki 14. *Geoarchaeology* **2024**, *39*, 143–167. [CrossRef]
20. Jia, Y.; Zhang, Y.Z.; Huang, C.C.; Wang, N.L.; Qiu, H.J.; Wang, H.Y.; Xiao, Q.L.; Chen, D.; Lin, X.; Liu, C.H. Weathering and Pedogenesis of the Late Pleistocene and Holocene Aeolian Loess-Paleosol Sections in the Yellow River Source Area, NE Tibetan Plateau. *Palaeogeogr. Palaeoclimatol. Palaeoecol.* **2022**, *600*, 111065. [CrossRef]
21. Rezende, S.B.D.; Franzmeier, D.P.; Resende, M.; Mancini, M.; Curi, N. Pedogenic Processes in a Chronosequence of Very Deeply Weathered Soils in Southeastern Brazil. *Catena* **2022**, *215*, 106362. [CrossRef]
22. Liu, C.C.; Dupont-Nivet, G.; Wang, W.; Deng, C.L. Magnetic Response to Pedogenesis in Aerobic Soils of Different Weathering Degree. *Palaeogeogr. Palaeoclimatol. Palaeoecol.* **2021**, *567*, 110240. [CrossRef]
23. Harnois, L. The C.I.W. index: A New Chemical Index of Weathering. *Sedim. Geol.* **1988**, *55*, 319–322. [CrossRef]
24. Nesbitt, H.W. Mobility and Fractionation of Rare Earth Elements During Weathering of Granodiorite. *Nature* **1979**, *279*, 206–210. [CrossRef]

25. Nesbitt, H.W.; Young, G.M. Early Proterozoic Climates and Plate Motions Inferred from Major Element Chemistry of Lutites. *Nature* **1982**, *299*, 715–717. [CrossRef]
26. Moghbeli, Z.; Owliaie, H.; Adhami, E.; Najafi-Ghiri, M.; Sanjari, S. Pedogenesis and Spatial Distribution of Soil Magnetic Properties along a Lithotoposequence in an Arid Region of Southern Iran. *Catena* **2021**, *198*, 104979. [CrossRef]
27. Chen, L.M.; Zhang, G.L.; Rossiter, D.G.; Cao, Z.H. Magnetic Depletion and Enhancement in the Evolution of Paddy and Non-paddy Soil Chronosequences. *Eur. J. Soil Sci.* **2015**, *66*, 886–897. [CrossRef]
28. César De Mello, D.; Demattê, J.A.M.; Silvero, N.E.Q.; Di Raimo, L.A.D.L.; Poppiel, R.R.; Mello, F.A.O.; Souza, A.B.; Safanelli, J.L.; Resende, M.E.B.; Rizzo, R. Soil Magnetic Susceptibility and Its Relationship with Naturally Occurring Processes and Soil Attributes in Pedosphere, in a Tropical Environment. *Geoderma* **2020**, *372*, 114364. [CrossRef]
29. Wang, S.Y. The Red Earth in Southern China: Its Magnetic Characters, Origins and Pedogenic Implication. Ph.D. Thesis, Zhejiang University, Hangzhou, China, 2014.
30. Li, F.R. Study on Soil Magnetic Characteristics and Its Relationship with Soil Formation Process Under Typical Climatic Zones in Yunnan. Master's Thesis, Kunming University of Science and Technology, Kunming, China, 2021.
31. Wang, M.C.; Li, H.X.; Zhang, X.L.; Wang, J.M.; Ye, J.M.; Zhang, M.H. Comparation of Magnetic Characteristics of Forest and Farmland Topsoils and Their Relationship with Environmental Factors. *Soils* **2025**, *57*, 716–724. [CrossRef]
32. Yuan, J.; Liu, J.K.; Zheng, R.H.; Shen, J.L. Studies on Characteristics of High-Energy Polarized Energy-Dispersive X-ray Fluorescence Spectrometer and Determination of Major and Trace Elements in Geological Samples. *Rock Miner. Anal.* **2020**, *39*, 816–827. [CrossRef]
33. Costa Filho, L.M.; Dobereiner, L.; de Campos, T.M.P.; Vargas, E. Fabric and engineering properties of saprolites and laterites. In Proceedings of the 12th International Symposium on Field Monitoring in Geomechanics, Rio de Janerio, Brazil, 13–18 August 1989; Volume 4, pp. 2463–2476.
34. Roddaz, M.; Viers, J.; Brusset, S.; Baby, P.; Hérail, G. Controls on weathering and provenance in the Amazonian foreland basin: Insights from major and trace element geochemistry of Neogene Amazonian sediments. *Chem. Geol.* **2006**, *226*, 31–65. [CrossRef]
35. Kanu, M.O.; Meludu, O.C.; Basavaiah, N.; Joseph, G. The Use of Environmental Magnetic Properties, Elemental Analysis and Geostatistical Tools for Soil Pollution Assessment, a Lesson from Takum, Nigeria. *Phys. Chem. Earth.* **2023**, *130*, 103377. [CrossRef]
36. Wang, G.Y.; Zhang, S.R.; Xiao, L.Y.; Zhong, Q.M.; Li, L.X.; Xu, G.R.; Deng, O.O.; Pu, Y.L. Heavy Metals in Soils from a Typical Industrial Area in Sichuan, China: Spatial Distribution, Source Identification and Ecological Risk Assessment. *Environ. Sci. Pollut. Res.* **2017**, *24*, 16618–16630. [CrossRef] [PubMed]
37. Ma, J.L.; Wei, G.J.; Xu, Y.G.; Liang, X.R.; Ma, Z.H.; Sun, W.D. Mobilization and re-distribution of major and trace elements during extreme weathering of basalt in Hainan Island, South China. *Geochim. Cosmochim. Acta* **2007**, *71*, 3223–3237. [CrossRef]
38. Chen, T.Y.; Lv, B.; Li, J.W.; Tang, J.H.; Zhang, S.L.; Jiang, S.Y. The applicability of Chemical Index of Alteration (CIA) to reflect weathering intensity of humid subtropical weathering crust soil. *Quat. Sci.* **2024**, *44*, 551–562. [CrossRef]
39. Feng, Z.G.; Wang, S.J.; Sun, C.X. Discussion on possible causes of increases in Si/Al ratio in surface layers of some lateritic profiles. *Geol. Geochem.* **2002**, *30*, 7–14. [CrossRef]
40. Zhu, H.J.; Chen, J.F.; Chen, S.L. *Soil Geography*, 3rd ed.; Higher Education Press: Beijing, China, 2019.
41. Tauseef, M.; Ray, E.; Paul, D.; Malik, J.N.; Ahmad, I. Mineralogical, Geochemical, and Magnetic Susceptibility Variations in the Loess-Paleosol Sequence from Pattan, Kashmir Valley, India Record an Enhanced Indian Summer Monsoon around 35 Ka. *Quat. Int.* **2022**, *616*, 55–66. [CrossRef]
42. Jordanova, D.; Jordanova, N.; Atanasova, A.; Tsacheva, T.; Petrov, P. Soil Tillage Erosion Estimated by Using Magnetism of Soils—A Case Study from Bulgaria. *Environ. Monit. Assess.* **2011**, *183*, 381–394. [CrossRef]
43. Hrouda, F. Models of Frequency-Dependent Susceptibility of Rocks and Soils Revisited and Broadened. *Geophys. J. Int.* **2011**, *187*, 1259–1269. [CrossRef]
44. Ouallali, A.; Bouhsane, N.; Bouhlassa, S.; Spalevic, V.; Kader, S.; Michael, R.; Sestras, P. Exploring soil pedogenesis through frequency-dependent magnetic susceptibility in varied lithological environments. *Euro-Mediterr. J. Environ. Integr.* **2024**, *10*, 887–900. [CrossRef]
45. Zhang, X.; Li, G.; Li, H.; Yang, T.; Chen, Y.; Ren, E.; Hu, J.; Yang, W. Relationship between magnetic properties and weathering in red soil profiles developed on weakly magnetic parent rock in the tropical and subtropical region of Yunnan, China. *Acta Geophys.* **2024**, *72*, 4063–4077. [CrossRef]
46. Bouhlassa, S.; Bouhsane, N. Assessment of the Impacts of Land-Use Change and Slope Position on Soil Loss by Magnetic Susceptibility-Based Models. *Int. J. Sediment Res.* **2023**, *38*, 455–468. [CrossRef]
47. Maher, B.A. The magnetic properties of Quaternary aeolian dusts and soils, and their palaeoclimatic significance. *Quat. Sci. Rev.* **2011**, *3*, 87–144. [CrossRef]
48. Liu, Q.; Roberts, A.P.; Larrasoaña, J.C.; Banerjee, S.K.; Guyodo, Y.; Tauxe, L.; Oldfield, F. Environmental magnetism: Principles and applications. *Earth-Sci. Rev.* **2012**, *50*, 2012RG000393. [CrossRef]

49. Torrent, J.; Liu, Q.; Barrón, V. Magnetic enhancement is linked to iron mineral transformations during pedogenesis. *Geoderma* **2006**, *33*, L02401. [CrossRef]
50. Xu, N.; Liu, G.X.; Tan, Q.F. High-Fidelity Far-Field Microscopy at λ/8 Resolution. *Laser Photonics Rev.* **2022**, *16*, 2200307. [CrossRef]
51. Xu, N.; Liu, G.X.; Tan, Q.F. Adjustable super-resolution microscopy with diffractive spot array illumination. *Appl. Phys. Lett.* **2020**, *116*, 254103. [CrossRef]

Disclaimer/Publisher's Note: The statements, opinions and data contained in all publications are solely those of the individual author(s) and contributor(s) and not of MDPI and/or the editor(s). MDPI and/or the editor(s) disclaim responsibility for any injury to people or property resulting from any ideas, methods, instructions or products referred to in the content.